CHEMISTRY OF MATERIALS

Communication

pubs.acs.org/cm

Broadband Emission with a Massive Stokes Shift from Sulfonium Pb−Br Hybrids

Matthew D. Smith,[†] Brian L. Watson,[‡] Reinhold H. Dauskardt,[‡] and Hemamala I. Karunadasa*,[†]

[†]Departments of Chemistry and [‡]Materials Science and Engineering, Stanford University, Stanford, California 94305, United States

Supporting Information

Organic−inorganic hybrids combine the electronic diversity of inorganic solids with the tunability of organic molecules. Indeed, the diversity of structures and photophysical properties in the family of organic−inorganic perovskites[1] fulfill the promise of hybrid materials. The three-dimensional (3D) lead-halide perovskites are under intense study as next-generation solar-cell absorbers,[2,3] while two-dimensional (2D) perovskites have been explored in phosphor,[4] light-emitting diode,[5,6] and photovoltaic[7] applications. Although lead-halide hybrids that exhibit the 3D or 2D perovskite structure of corner-sharing metal-halide octahedra have received the most recent attention, there are a large number of halometalate bonding motifs and structure archetypes[8] whose optical properties have not been explored in comparable detail. We replaced ammonium cations with sulfonium cations to access a 2D Pb−Br structure with unusual optical properties. Upon ultraviolet (UV) excitation, the layered solid $(tms)_4Pb_3Br_{10}$ (**1**, tms = trimethylsulfonium; $(CH_3)_3S^+$) emits broad red/near-infrared photoluminescence (PL) with a very large Stokes shift of 1.7 eV. We ascribe this PL to self-trapped excitonic emission, in analogy with our recent discovery of broadband, white-light emission in 2D lead-halide perovskites.[9,10] Herein, we extend low-dimensional hybrids that exhibit broad PL to a new family of materials.

The 3D and 2D hybrid perovskites feature organoammonium cations, whose protic nature has been implicated in their moisture and thermal instability.[11] Moving beyond the perovskite framework to less-explored topologies, and employing a more diverse library of main-group cations[12,13] can expand the phase space of these hybrid semiconductors. In particular, hydrogen-bonding interactions are important templating agents for layered lead-halide perovskites,[14] and their absence may also provide a route to trigger the formation of novel inorganic structures with new optical and electronic properties. Although the organoammonium cations in 2D perovskites can feature sulfur-containing groups such as disulfides,[15] to our knowledge, **1** is the first 2D lead-halide hybrid to contain sulfonium cations. Lower-dimensional metal-halide hybrids containing trimethylsulfonium have been reported.[16,17]

Slow diffusion of diethyl ether into a solution of dimethylformamide (DMF) and dimethyl sulfoxide (DMSO) containing trimethylsulfonium bromide ($(CH_3)_3SBr$) and $PbBr_2$ yields colorless crystals of **1**. Solid **1** crystallizes in the monoclinic space group $P2_1/n$ with alternating layers of Pb−Br sheets and trimethylsulfonium cations (Figure 1A). The Pb−Br sheets contain trimers of face-sharing octahedra linked through bridging bromides to adjacent trimers (Figure 1B), analogous with the structure of $Cs_4Mg_3F_{10}$.[18] The inorganic sublattice is also isostructural with the previously reported Pb−Br hybrid $(tmpa)_4Pb_3Br_{10}$ (**2**; tmpa = trimethylphenylammonium).[19]

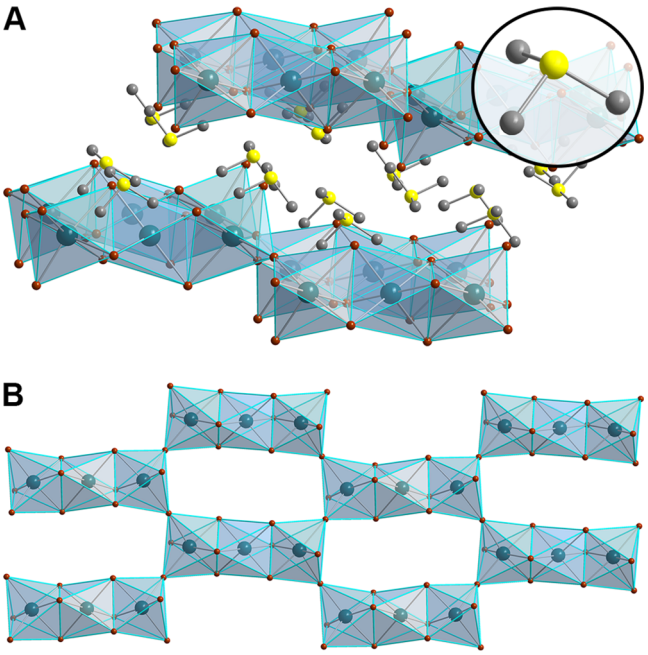

Figure 1. (A) X-ray crystal structure of $(tms)_4Pb_3Br_{10}$ (**1**, tms = trimethylsulfonium; $(CH_3)_3S^+$). Inset: the tms cation. (B) Top-down view of the inorganic layers in **1**. Green, brown, yellow, and gray spheres represent Pb, Br, S, and C atoms, respectively. Disordered and H atoms removed for clarity.

Upon photoexcitation by 375 nm or higher-energy UV light, both **1** and **2** exhibit broad red PL at room temperature that extends into the near-infrared region (Figure 2A,B). The emission is extremely broad, with a peak wavelength of 685 nm, emission width of ca. 2 eV, and full width at half-maximum of ca. 0.7 eV. The CIE chromaticity coordinates[20,21] for **1** are (0.55, 0.41). The emission also contains a small higher-energy shoulder with an onset of ca. 390 nm (Figure S1A). Though we were unable to grow thin films of **1** for transmission measurements, diffuse-reflectance measurements converted to pseudoabsorption spectra using the Kubelka−Munk function[22] reveal that the PL exhibits a massive Stokes shift of ca. 1.7 eV from the absorption onset. This is more than 40% larger than the ca. 1.2 eV Stokes shift observed in the prototypical white-

Received: June 22, 2017
Revised: August 15, 2017
Published: August 17, 2017

ACS Publications © 2017 American Chemical Society

DOI: 10.1021/acs.chemmater.7b02594
Chem. Mater. 2017, 29, 7083−7087

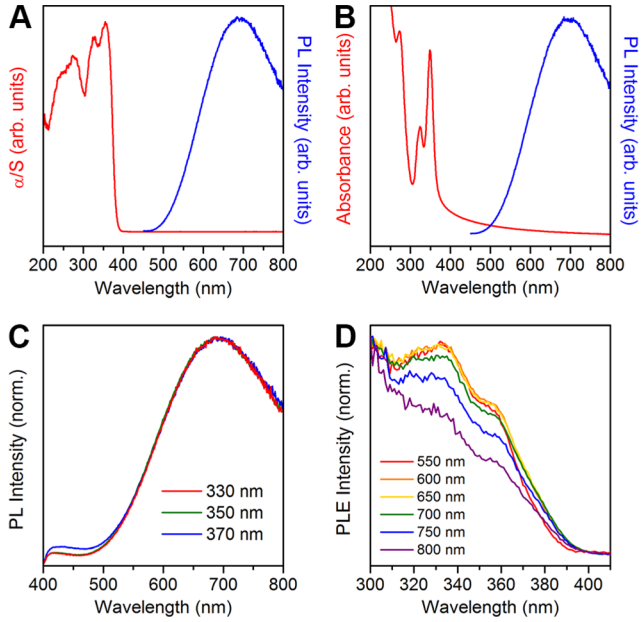

Figure 2. (A) Diffuse reflectance data transformed using the Kubelka–Munk (K-M) function (α and S are the absorption and scattering coefficients, respectively)[22] and photoluminescence (PL) spectrum with an excitation wavelength (λ_{ex}) of 350 nm for powdered $(tms)_4Pb_3Br_{10}$(**1**). (B) Thin-film optical absorbance and PL spectra with λ_{ex} = 350 nm for $(tmpa)_4Pb_3Br_{10}$ (**2**). (C) Excitation-wavelength-dependent PL spectra of **1** and (D) emission-wavelength-dependent photoluminescence excitation (PLE) spectra of **1**.

light-emitting 2D perovskite $(EDBE)PbBr_4$ (EDBE = 2,2′-(ethylenedioxy)bis(ethylammonium); see Table S8 for the Stokes shifts of selected Pb–Br hybrids).[10]

We successfully deposited thin films of **2** using spin-coating, producing transparent films where the inorganic layers are preferentially oriented parallel to the substrate, similar to 2D perovskites.[1] Transmission measurements on thin films of **2** exhibit a strong, sharp resonance at 349 nm (3.55 eV; Figures 2B and S2), which we ascribe to free excitons (photogenerated electron–hole pairs), analogous to 2D lead-halide perovskites[23,24] and lead halides.[25] This resonance is clearly separated from the continuum absorption features, suggesting that excitons are tightly bound. Two main effects serve to cooperatively enhance the exciton binding energy (attraction between the electron and hole in an exciton, E_b) in layered organic–inorganic materials: quantum and dielectric confinement. Quantum confinement of the excitonic wave function is a result of the 2D structure of the inorganic layers and leads to a 4-fold enhancement of E_b over a comparable 3D material.[23,24] The low dielectric constant of the organic layers[26] poorly screens the Coulombic attraction between the exciton's electron and hole, further enhancing E_b through dielectric confinement. Free-excitonic luminescence typically exhibits a narrow bandwidth and minimal Stokes shift (ca. 10–20 meV in 2D Pb–Br perovskites).[27] Upon UV photoexcitation at room temperature, the broad, Stokes-shifted emission dominates the PL spectra of **1** and **2** rather than free-exciton PL, similar to the broad components of the PL in the white-light-emitting perovskites $(N\text{-MEDA})PbBr_4$ (N-MEDA = N^1-methylethane-1,2-diammonium) and $(EDBE)PbBr_4$.[9,10]

Our mechanistic studies on the white-light-emitting perovskites[28] implicated exciton self-trapping as the cause of this unusual PL. Typically, layered lead-halide perovskites exhibit strong, narrow luminescence at room temperature[4] owing to the radiative recombination of strongly bound free excitons.[24] When the free exciton couples strongly to the inorganic lattice, it is stabilized in energy or self-trapped in distortions induced by its own interaction with the lattice. Exciton or carrier self-trapping is common in polar semiconductors or dielectrics, such as the lead(II) halides,[29] alkali halides,[30] and molecular organic semiconductors such as pyrene.[31] We therefore hypothesized that the broad red PL we observe in **1** and **2** is due to radiative recombination of self-trapped excitons, in analogy to 2D lead-halide perovskites.[9,10,28]

Exciton self-trapping in 2D lead-halide perovskites has a significant component that is intrinsic to the bulk crystal structure of the material.[10,28,32] However, extrinsic phenomena such as defects or dopants[33,34] can also contribute substantially to PL broadening. In **1**, the shape of the broad PL appears invariant of the excitation energy above 370 nm (Figure 2C). Additionally, photoluminescence excitation (PLE) spectra probing the broad emission from 550 to 800 nm in **1** exhibit the same shape and features (Figure 2D). Therefore, the same excited states contribute to the entirety of the observed broad emission. The PLE and diffuse reflectance data exhibit similar onsets at ca. 390–400 nm, evidence that the PL has a strong intrinsic element. In contrast, the weak, higher-energy shoulder appears to stem from subgap states as evident in the PLE spectrum (Figure S1B), possibly a result of permanent material defects.

The PL of **2** is similar to that of **1**, except that subgap states appear to generate stronger emission features. Upon exciting at wavelengths shorter than 360 nm, **2** exhibits broadband red PL nearly identical to **1**. However, excitation in the wavelength range of 370–450 nm causes **2** to strongly emit broadband, green-white light (Figure 3B). The CIE chromaticity

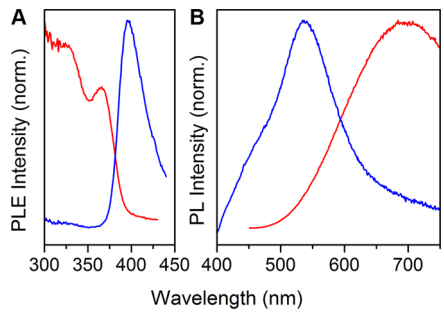

Figure 3. (A) Normalized photoluminescence excitation (PLE) spectra for $(tmpa)_4Pb_3Br_{10}$ (**2**) at emission wavelengths of 490 nm (blue) and 700 nm (red). (B) Normalized photoluminescence (PL) spectra for **2** with excitation wavelengths of 390 nm (blue) and 350 nm (red).

coordinates[20] of this PL (0.32, 0.45) are closer to that of pure white light (0.33, 0.33), compared to the red PL of **1**. The PLE spectra of **2** show a large peak at ca. 400 nm for this green-white PL (Figure 3A). This feature is below the energies for substantial absorption in the diffuse reflectance and transmission UV–Vis spectra of **2** (Figures 2B and S2). We hypothesize that permanent material defects may be involved with this emission, which is likely related to the shoulder in the PL spectrum of **1**.

We collected time-resolved photoluminescence (TRPL) spectra at room temperature on both a collection of large crystals and powders of **1** (Figure 4A). Biexponential fits to

DOI: 10.1021/acs.chemmater.7b02594
Chem. Mater. 2017, 29, 7083–7087

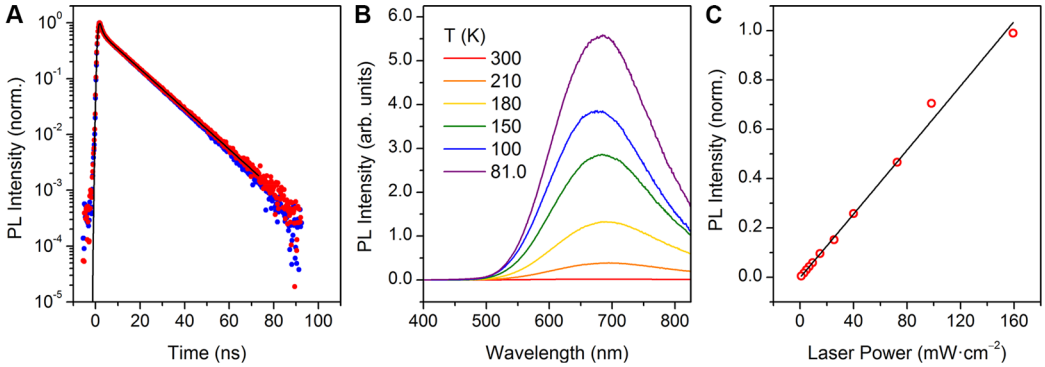

Figure 4. (A) Time-resolved photoluminescence (PL) traces for powders (red) and crystals (blue) of $(tms)_4Pb_3Br_{10}$ (**1**) with the fit (black) to the data, with an excitation wavelength (λ_{ex}) of 365 nm. (B) Temperature-dependent static PL of **1** (λ_{ex} = 355 nm). (C) Power-dependent PL (λ_{ex} = 375 nm) intensity of crystals of **1** (red circles) and fit to the data (black line).

these data show contributions from both a fast decay with a time constant τ_1 faster than the instrument response (ca. 1.20 ns) and a much longer process with $\tau_{2,crystals}$ = 11.82(2) ns and $\tau_{2,powder}$ = 12.01(2) ns. Despite the larger surface area of the powder compared to the crystal sample, the relative ratio of the two fit pre-exponential factors in each sample is essentially identical, suggesting that particle surface states do not play a large role in the observed PL. Furthermore, the long lifetimes of the broad emission here are comparable to that of the (110) white-light-emitting perovskite $(EDBE)PbBr_4$, which was measured as 14(1) ns.[10]

Intensity-dependent continuous-wave PL measurements also support an intrinsic, excitonic origin to the broad red PL. In crystals of **1**, the integrated PL intensity increases linearly with increasing excitation intensity ($y = y_0 + ax^b$; where a = 6.20(9) $\times 10^{-3}$, b = 1.009(4), y_0 = 1(2) $\times 10^{-4}$ for crystals; Figure 4C). A linear or slightly superlinear power dependence is typically observed for excitonic[35] recombination, and is predicted by theory.[36] Free-carrier luminescence is expected to exhibit a quadratic dependence on excitation intensity owing to its bimolecular nature, whereas emission involving permanent defects is sublinear in excitation intensity.[36] The power-dependence of the broad emissions across a range of lead-halide hybrids, including 2D perovskites[10,32,37] and 1D chain structures,[38] exhibit linear or nearly linear behavior. We also synthesized **1** under air- and moisture-free conditions, and still observed the red PL. In contrast, air or moisture exposure have been previously suggested to yield a weak broad red emission at low temperatures in $Cs_3Bi_2Br_9$ through the formation of Bi−O defects.[39] Upon cooling from room temperature to 80 K, the broad PL peak in **1** narrows significantly and increases in intensity (Figure 4B). Given the similarity of both the static and dynamic characteristics of the PL in **1** and **2** to that of the white-light-emitting perovskites, we propose that exciton self-trapping is a feature intrinsic to the layered $[Pb_3Br_{10}]^{4-}$ lattice.

Similar to perovskites that can feature both mono- and diammonium cations, we then attempted to expand the family of sulfonium Pb−Br hybrids by using the disulfonium cation $(CH_3)_2S(CH_2)_4S(CH_3)_2^{2+}$ (hereafter 1,4-bbdms). Addition of 1,4-bbdms to a solution of $PbBr_2$ dissolved in a mixture of DMF and DMSO leads to the cocrystallization of two novel sulfonium lead bromides. The compounds $(1,4\text{-bbdms})_3Pb_3Br_{12}$ (**3a**) and $(1,4\text{-bbdms})_4Pb_5Br_{18}\cdot DMF_{0.7}DMSO_{1.3}$ (**3b**) represent members of an extended family of sulfonium lead halides (Figures 5A and S3). Here, the inorganic components are isolated trimers and pentamers of face-sharing Pb−Br octahedra, respectively. The $Pb_3Br_{12}^{6-}$ trimers in **3a** can be considered the building block of the Pb−Br layers in **1**, analogous to the $PbBr_6^{4-}$ octahedron for the perovskite structures. We separately synthesized phase-pure powders of **3a** (details in the Supporting Information). Diffuse reflectance measurements reveal an absorption peak of 328 nm, ca. 290 meV higher than that of **1**. Similar to **1**, under UV illumination, **3a** also exhibits broad red PL with maximum intensity at 690 nm. Also as in **1**, the PLE spectra of this red PL in **3a** appear similar to its diffuse reflectance spectrum (Figure S4). The two higher-energy and lower-intensity PL bands at ca. 375 and 460 nm may be from bound free excitons or defects. In fact, the PLE spectra of the 460 nm feature reveals significant intensity below the absorption onset (Figure S5), similar to the case of both **1** and **2**.

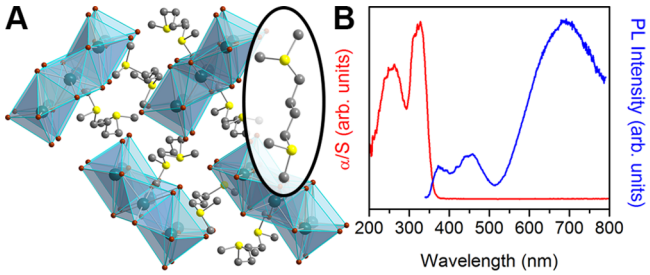

Figure 5. (A) Crystal structure of $(1,4\text{-bbdms})_3Pb_3Br_{12}$ (**3a**; 1,4-bbdms = $(CH_3)_2S(CH_2)_4S(CH_3)_2^{2+}$). Inset: the 1,4-bbdms cation. (B) Diffuse reflectance data transformed using the Kubelka−Munk function[22] (α and S are the absorption and scattering coefficients, respectively) and PL spectrum for powdered **3a** (blue). Green, brown, yellow, and gray spheres represent Pb, Br, S, and C atoms, respectively. H atoms removed for clarity.

Herein, we demonstrate that the broad, Stokes-shifted PL of lead-halide hybrids is not constrained to ammonium-based compounds, with the synthesis of a family of sulfonium-based hybrids. Through steady-state and time-dependent fluorescence measurements, we ascribe the broadband PL primarily to the radiative recombination of self-trapped excitons. Though we cannot entirely eliminate permanent-defect-mediated mechanisms, our studies suggest that the red PL is mostly intrinsic to these hybrids. Interestingly, the connectivity of the Pb−Br component, rather than bandgap or exciton energy, appears to influence the color of the broad PL. Here, we observe that face-sharing Pb−Br octahedra afford broad red emission peaked at ca. 700 nm for both 2D and 0D structures. In contrast, the corner-sharing connectivity of the perovskite broad emitters

DOI: 10.1021/acs.chemmater.7b02594
Chem. Mater. 2017, 29, 7083−7087

yields yellow-to-white[9,10,32,37,40,41] emission, despite large (>0.5 eV) variations in exciton absorption energy. The broad PL's dependence on local connectivity, above other factors such as dimensionality or bandgap, supports the self-trapping mechanism, which is based on localized distortions in the inorganic sublattice. If exciton self-trapping is indeed an intrinsic property of this material, then the very large Stokes shift implies correspondingly large-amplitude structural distortions associated with the self-trapped exciton.[34] Achieving more diverse connectivity and inorganic bonding motifs templated by uncommon cations offers the opportunity to further expand, understand, and control the emission from metal-halide hybrids.

■ ASSOCIATED CONTENT

Supporting Information

The Supporting Information is available free of charge on the ACS Publications website at DOI: 10.1021/acs.chemmater.7b02594.

Experimental details, crystallographic information, and spectra (PDF)

Data for $(tms)_4Pb_3Br_{10}$ (CIF)

Data for $(1,4\text{-bbdms})_3Pb_3Br_{12}$ (CIF)

Data for $(1,4\text{-bbdms})_4Pb_5Br_{18}\cdot DMF_{0.7}DMSO_{1.3}$ (CIF)

■ AUTHOR INFORMATION

Corresponding Author

*hemamala@stanford.edu

ORCID

Matthew D. Smith: 0000-0002-4197-5176

Hemamala I. Karunadasa: 0000-0003-4949-8068

Notes

The authors declare no competing financial interest.

The CIFs for $(tms)_4Pb_3Br_{10}$, $(1,4\text{-bbdms})_3Pb_3Br_{12}$, and $(1,4\text{-bbdms})_4Pb_5Br_{18}\cdot DMF_{0.7}DMSO_{1.3}$ have been deposited in the Cambridge Crystallographic Data Centre under deposition numbers 1557449, 1557450, and 1557451, respectively.

■ ACKNOWLEDGMENTS

This research was supported by the Alfred P. Sloan Fellowship, and the Stanford Terman and Gabilan Faculty Fellowships. M.D.S. is supported by a National Science Foundation (NSF) Graduate Research Fellowship (DGE-114747). We are grateful to Prof. M. D. McGehee for access to equipment. Single-crystal XRD studies were performed at beamline 11.3.1 at the Advanced Light Source (ALS) at the Lawrence Berkeley National Laboratory. The ALS is supported by the Director, Office of Science, Office of Basic Energy Sciences, of the U.S. Department of Energy (Contract No. DE-AC02-05CH11231). PL lifetime analysis was conducted at the Molecular Analysis Facility, a National Nanotechnology Coordinated Infrastructure site at the University of Washington, which is supported in part by the NSF (grant ECC-1542101), the University of Washington, the Molecular Engineering & Sciences Institute, the Clean Energy Institute, and the National Institutes of Health. Part of this work used the Stanford Nano Shared Facilities (SNSF), supported by the NSF (award ECCS-1542152).

■ REFERENCES

(1) Mitzi, D. B. In *Prog. Inorg. Chem.*; Karlin, K. D., Ed.; John Wiley & Sons Inc: New York, 1999; Vol. *48*, pp 1−121.

(2) Kojima, A.; Teshima, K.; Shirai, Y.; Miyasaka, T. Organometal Halide Perovskites as Visible-Light Sensitizers for Photovoltaic Cells. *J. Am. Chem. Soc.* **2009**, *131*, 6050−6051.

(3) Snaith, H. J. Perovskites: The Emergence of a New Era for Low-Cost, High-Efficiency Solar Cells. *J. Phys. Chem. Lett.* **2013**, *4*, 3623−3630.

(4) Gauthron, K.; Lauret, J.-S.; Doyennette, L.; Lanty, G.; Al Choueiry, A.; Zhang, S. J.; Brehier, A.; Largeau, L.; Mauguin, O.; Bloch, J.; Deleporte, E. Optical Spectroscopy of Two-Dimensional Layered $(C_6H_5C_2H_4\text{-}NH_3)_2\text{-}PbI_4$ Perovskite. *Opt. Express* **2010**, *18*, 5912−5919.

(5) Hattori, T.; Taira, T.; Era, M.; Tsutsui, T.; Saito, S. Highly Efficient Electroluminescence From a Heterostructure Device Combined with Emissive Layered-Perovskite and an Electron-Transporting Organic Compound. *Chem. Phys. Lett.* **1996**, *254*, 103−108.

(6) Chondroudis, K.; Mitzi, D. B. Electroluminescence from an Organic-Inorganic Perovskite Incorporating a Quaterthiophene Dye Within Lead Halide Perovskite Layers. *Chem. Mater.* **1999**, *11*, 3028−3030.

(7) Smith, I. C.; Hoke, E. T.; Solis-Ibarra, D.; McGehee, M. D.; Karunadasa, H. I. A Layered Hybrid Perovskite Solar-Cell Absorber with Enhanced Moisture Stability. *Angew. Chem., Int. Ed.* **2014**, *53*, 11232−11235.

(8) Mercier, N.; Louvain, N.; Bi, W. Structural Diversity and Retro-Crystal Engineering Analysis of Iodometalate Hybrids. *CrystEngComm* **2009**, *11*, 720−734.

(9) Dohner, E. R.; Hoke, E. T.; Karunadasa, H. I. Self-Assembly of Broadband White-Light Emitters. *J. Am. Chem. Soc.* **2014**, *136*, 1718−1721.

(10) Dohner, E. R.; Jaffe, A.; Bradshaw, L. R.; Karunadasa, H. I. Intrinsic White-Light Emission from Layered Hybrid Perovskites. *J. Am. Chem. Soc.* **2014**, *136*, 13154−13157.

(11) Slavney, A. H.; Smaha, R. W.; Smith, I. C.; Jaffe, A.; Umeyama, D.; Karunadasa, H. I. Chemical Approaches to Addressing the Instability and Toxicity of Lead−Halide Perovskite Absorbers. *Inorg. Chem.* **2017**, *56*, 46−55.

(12) Krautscheid, H.; Lode, C.; Vielsack, F.; Vollmer, H. Synthesis and Crystal Structures of Iodoplumbate Chains, Ribbons and Rods with New Structural Types. *J. Chem. Soc., Dalton Trans.* **2001**, 1099−1104.

(13) Gröger, H.; Lode, C.; Vollmer, H.; Krautscheid, H.; Lebedkin, S. Bromoplumbate mit Kettenförmigen und Isolierten Anionen: $(Bzl_4P)_2[Pb_3Br_8]$, $(Bzl_4P)_2[Pb_3Br_8(dmf)_2]$, $(Bzl_4P)[PbBr_3]$, $(Bzl_4P)_2[PbBr_4]$ und $(Bzl_4P)_4[Pb_2Br_6][PbBr_4]$. *Z. Anorg. Allg. Chem.* **2002**, *628*, 57−62.

(14) Mercier, N.; Poiroux, S.; Riou, A.; Batail, P. Unique Hydrogen Bonding Correlating with a Reduced Band Gap and Phase Transition in the Hybrid Perovskites $(HO(CH_2)_2NH_3)_2PbX_4$ (X = I, Br). *Inorg. Chem.* **2004**, *43*, 8361−8366.

(15) Lemmerer, A.; Billing, D. G. Effect of Heteroatoms in the Inorganic−Organic Layered Perovskite-Type Hybrids $[(ZC_nH_{2n}NH_3)_2PbI_4]$, n = 2, 3, 4, 5, 6; Z = OH, Br and I; and $[(H_3NC_2H_4S_2C_2H_4NH_3)PbI_4]$. *CrystEngComm* **2010**, *12*, 1290−1301.

(16) Ikeda, R.; Nakamura, D.; Kadel, R.; Weiss, A. The Trimethylsulfonium Ion, $[(CH_3)_3S]^{\oplus}$, in Hexachlorometallate(IV) Complexes, $[(CH_3)_3S]_2MCl_6$ (M = Pt, Se, Te, Sn). ^1H NMR, ^{35}Cl NQR, and X-Ray Diffraction Studies. *Ber. Bunsen-Ges.* **1983**, *87*, 570−574.

(17) Kaltzoglou, A.; Stoumpos, C. C.; Kontos, A. G.; Manolis, G. K.; Papadopoulos, K.; Papadokostaki, K. G.; Psycharis, V.; Tang, C. C.; Jung, Y.-K.; Walsh, A.; Kanatzidis, M. G.; Falaras, P. Trimethylsulfonium Lead Triiodide: An Air-Stable Hybrid Halide Perovskite. *Inorg. Chem.* **2017**, *56*, 6302−6309.

(18) Steinfink, H.; Brunton, G. D. The Crystal Structure of $Cs_4Mg_3F_{10}$. *Inorg. Chem.* **1969**, *8*, 1665−1668.

DOI: 10.1021/acs.chemmater.7b02594
Chem. Mater. 2017, 29, 7083−7087

(19) Wiest, T.; Blachnik, R.; Reuter, H. Crystal Structure of $[PhMe_3N]_4[Pb_3Br_{10}]$. *Z. Naturforsch. (B)* **1999**, *54*, 1099−1102.
(20) Ye, S.; Xiao, F.; Pan, Y. X.; Ma, Y. Y.; Zhang, Q. Y. Phosphors in Phosphor-Converted White Light-Emitting Diodes: Recent Advances in Materials, Techniques and Properties. *Mater. Sci. Eng., R* **2010**, *71*, 1−34.
(21) Selverian, J. *ColorCalculator*, 7.15 ed.; OSRAM Sylvania, Inc.: Beverly, MA, 2017.
(22) Kubelka, P.; Munk, F. Ein Beitrag zur Optik der Farbanstriche. *Z. Technol. Phys.* **1931**, *12*, 593−601.
(23) Ishihara, T. Optical Properties of PbI-Based Perovskite Structures. *J. Lumin.* **1994**, *60−61*, 269−274.
(24) Takagi, H.; Kunugita, H.; Ema, K. Influence of the Image Charge Effect on Excitonic Energy Structure in Organic-Inorganic Multiple Quantum Well Crystals. *Phys. Rev. B: Condens. Matter Mater. Phys.* **2013**, *87*, 125421.
(25) Fujita, M.; Itoh, M.; Bokumoto, Y.; Nakagawa, H.; Alov, D. L.; Kitaura, M. Optical Spectra and Electronic Structures of Lead Halides. *Phys. Rev. B: Condens. Matter Mater. Phys.* **2000**, *61*, 15731−15737.
(26) Muljarov, E. A.; Tikhodeev, S. G.; Gippius, N. A.; Ishihara, T. Excitons in Self-Organized Semiconductor/Insulator Superlattices: PbI-Based Perovskite Compounds. *Phys. Rev. B: Condens. Matter Mater. Phys.* **1995**, *51*, 14370−14378.
(27) Kitazawa, N. Excitons in Two-Dimensional Layered Perovskite Compounds: $(C_6H_5C_2H_4NH_3)_2Pb(Br,I)_4$ and $(C_6H_5C_2H_4NH_3)_2Pb(Cl,Br)_4$. *Mater. Sci. Eng., B* **1997**, *49*, 233−238.
(28) Hu, T.; Smith, M. D.; Dohner, E. R.; Sher, M.-J.; Wu, X.; Trinh, M. T.; Fisher, A.; Corbett, J.; Zhu, X.-Y.; Karunadasa, H. I.; Lindenberg, A. M. Mechanism for Broadband White-Light Emission from Two-Dimensional (110) Hybrid Perovskites. *J. Phys. Chem. Lett.* **2016**, *7*, 2258−2263.
(29) Iwanaga, M.; Azuma, J.; Shirai, M.; Tanaka, K.; Hayashi, T. Self-Trapped Electrons and Holes in $PbBr_2$ Crystals. *Phys. Rev. B: Condens. Matter Mater. Phys.* **2002**, *65*, 214306.
(30) Stoneham, A. M. Electronic Structure of the Self-Trapped Exciton in Sodium Chloride. *J. Phys. C: Solid State Phys.* **1974**, *7*, 2476−2486.
(31) Matsui, A.; Nishimura, H. Luminescence of Free and Self Trapped Excitons in Pyrene. *J. Phys. Soc. Jpn.* **1980**, *49*, 657−663.
(32) Smith, M. D.; Jaffe, A.; Dohner, E. R.; Lindenberg, A. M.; Karunadasa, H. I. Structural Origins of Broadband Emission from Layered Pb−Br Hybrid Perovskites. *Chem. Sci.* **2017**, *8*, 4497−4504.
(33) Nakahara, J.; Kobayashi, K. Edge Emissions and Broad Band Emissions in Thallous Halides. *J. Phys. Soc. Jpn.* **1976**, *40*, 180−188.
(34) Song, K. S.; Williams, R. T. *Self-Trapped Excitons*, 2nd ed.; Solid-State Sciences; Springer: Germany, 1996; Vol. *105*.
(35) Netzel, C.; Hoffmann, V.; Wernicke, T.; Knauer, A.; Weyers, M.; Kneissl, M.; Szabo, N. Temperature and Excitation Power Dependent Photoluminescence Intensity of GaInN Quantum Wells with Varying Charge Carrier Wave Function Overlap. *J. Appl. Phys.* **2010**, *107*, 033510.
(36) Schmidt, T.; Lischka, K.; Zulehner, W. Excitation-Power Dependence of the Near-Band-Edge Photoluminescence of Semiconductors. *Phys. Rev. B: Condens. Matter Mater. Phys.* **1992**, *45*, 8989−8994.
(37) Yangui, A.; Garrot, D.; Lauret, J. S.; Lusson, A.; Bouchez, G.; Deleporte, E.; Pillet, S.; Bendeif, E. E.; Castro, M.; Triki, S.; Abid, Y.; Boukheddaden, K. Optical Investigation of Broadband White-Light Emission in Self-Assembled Organic−Inorganic Perovskite $(C_6H_{11}NH_3)_2PbBr_4$. *J. Phys. Chem. C* **2015**, *119*, 23638−23647.
(38) Yuan, Z.; Zhou, C.; Tian, Y.; Shu, Y.; Messier, J.; Wang, J. C.; van de Burgt, L. J.; Kountouriotis, K.; Xin, Y.; Holt, E.; Schanze, K.; Clark, R.; Siegrist, T.; Ma, B. One-Dimensional Organic Lead Halide Perovskites with Efficient Bluish White-Light Emission. *Nat. Commun.* **2017**, *8*, 14051.
(39) Timmermans, C. W. M.; Blasse, G. On the Luminescence of $Cs_3Bi_2Br_9$ Single Crystals. *Phys. Status Solidi B* **1981**, *106*, 647−655.
(40) Mao, L.; Wu, Y.; Stoumpos, C. C.; Wasielewski, M. R.; Kanatzidis, M. G. White-Light Emission and Structural Distortion in New Corrugated Two-Dimensional Lead Bromide Perovskites. *J. Am. Chem. Soc.* **2017**, *139*, 5210−5215.
(41) Thirumal, K.; Chong, W. K.; Xie, W.; Ganguly, R.; Muduli, S. K.; Sherburne, M.; Asta, M.; Mhaisalkar, S.; Sum, T. C.; Soo, H. S.; Mathews, N. Morphology-Independent Stable White-Light Emission from Self-Assembled Two-Dimensional Perovskites Driven by Strong Exciton−Phonon Coupling to the Organic Framework. *Chem. Mater.* **2017**, *29*, 3947−3953.

DOI: 10.1021/acs.chemmater.7b02594
Chem. Mater. 2017, 29, 7083−7087